

Sensitivity analyses of a multi-physics long-term clogging model for steam generators

OpenTURNS Users' Day #17 @ EDF Lab Saclay

E. Jaber^{1,2,3}, V. Chabridon^{1,*}, E. Remy¹, M. Baudin¹, D. Lucor², M. Mousseot³, B. Iooss¹

June 14th, 2024

¹EDF R&D, 6 quai Watier, 78401 Chatou, France

²Université Paris-Saclay, CNRS, LISN, 91405, Orsay, France

³Université Paris-Saclay, CNRS, ENS Paris-Saclay, Centre Borelli, 91190, Gif-sur-Yvette, France

* Contact (first dot last at edf dot fr)

Foreword and acknowledgements

◆ Foreword

Edgar Jaber is involved in a PhD program (CIFRE EDF) funded by the French National Association for Technological Research (ANRT) under Grant n° 2022/1412.

◆ Acknowledgements

- Colleagues from EDF R&D: Qingqing Feng, Stéphane Pujet and Morgane Garo Sail (EDF R&D/MFEE Department)
- Colleagues from EDF Nuclear Division: Jérôme Delplace and Matthieu Wintergerst
- Régis Lebrun (Airbus) & the OT Dev' Team 🌟🌟

Introduction

Industrial context and motivations

◆ Industrial context

- ❑ Steam generators (SGs) ↳ heat exchangers found within pressurized water nuclear reactors (PWRs)
- ❑ PWRs consist of two distinct water circuits responsible for heat exchange
- ❑ This heated water then moves to the SG where it transfers its heat to the water in the secondary loops (usually ↳ 3 or 4 loops, i.e., 3 or 4 SGs).

Industrial context and motivations

◆ Industrial context

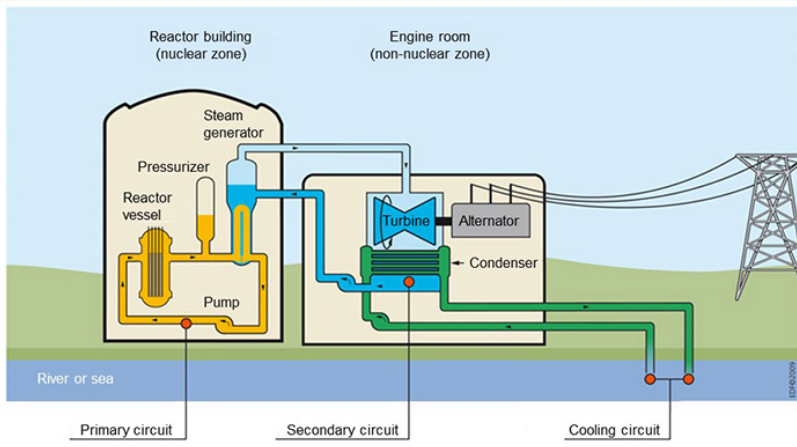


Figure 1: A typical French PWR (source: IRSN).

Industrial context and motivations

◆ Motivations

- ❑ The primary fluid circulates within a bundle of U-shaped tubes, which are stabilized by tube-support plates (TSPs)
- ❑ Adjacent to these tubes, the secondary fluid flows through the holes of the TSP and undergoes vaporization due to the heat from the primary fluid in the tubes.

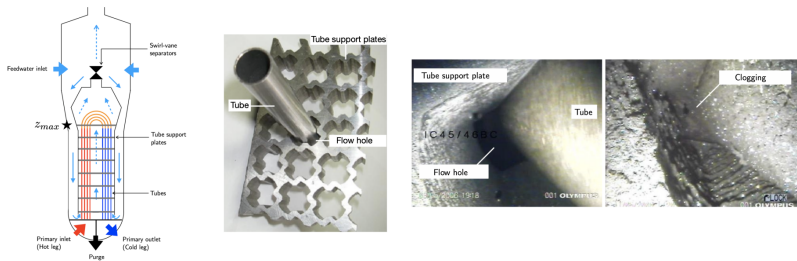


Figure 2: SG scheme, TSP and example of video examination during an PWR outage (© EDF).

Industrial context and motivations

◆ “A Taste of Clogging”

- ❑ After prolonged periods of operation \Rightarrow clogging phenomenon
- ❑ Clogging \Rightarrow reduction of the flow-holes area within the TSPs due to the accumulation of iron oxide deposits
- ❑ Deposits \Rightarrow primarily result from the corrosion of the secondary circuit (oxides carried by the secondary flow)
- ❑ Impacts on the SGs \Rightarrow causing a localized redistribution of flow among the TSP flow holes, increasing the risk of vibration, SG tube ruptures, and affecting the SGs' response to operational changes

Industrial context and motivations

◆ “A Taste of Clogging”

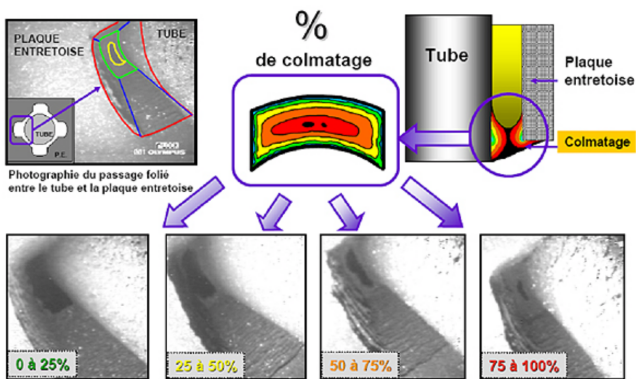


Figure 3: Clogging evaluation with non-destructive video (source: EDF - ASN).

◆ Main challenges

- ❑ How to address this issue? \Rightarrow measure/evaluate the clogging rate τ_c during PWR outages using non-destructive video examinations
- ❑ This clogging rate \Rightarrow average quantity that measures how much the holes of a TSP are clogged
- ❑ Preventive maintenance \Rightarrow consisting of heavy chemical cleaning processes
- ❑ Secondary fluid pH \Rightarrow monitored by chemical conditioning as part of the preventive measures
- ❑ Maintenance of such a component is complex and very costly \Rightarrow needs to be optimized w.r.t. several constraints (operational, safety, etc.)

Industrial context and motivations

◆ Main challenges



Figure 4: SG replacement (source: DR)

- ☞ Typical SG dimensions: 20 m (height), 4.5 m (diameter), 300 t

◆ Simulation tools available

- ❑ EDF R&D ↳ developed a numerical simulation chain known as “THYC-Puffer-DEPOTHYC” (“THYC-Puffer-DEPO” or TPD)
☞ initially proposed by [Pru12], then improved by [FNB⁺23]
- ❑ TPD ↳ spatiotemporal simulator, large number of inputs to fully model an entire SG and all the U-shaped tubes (geometric entries left as deterministic)
- ❑ TPD ↳ calibrated w.r.t. real in-situ data (scalar calibration parameter a_v)
- ❑ Only a few of the inputs are affected by uncertainties, either due to physical variability or a lack of knowledge about these physical quantities

Industrial context and motivations

◆ Motivations and objectives

- What about the literature on this subject? ↗ Not that much except... pioneering works of [Gir12], then [LSS⁺23]
 - In [LSS⁺23] ↗ almost similar study but with different UQ tools (neural network, Sobol' indices, Bayesian calibration)
 - But the computational model and output variable of interest are quite different!

☞ Main objectives of the talk

- Perform a full UQ analysis of the new TPD chain at a moderate cost
 - ↗ surrogate modeling
- Investigate, through sensitivity analysis (SA) the possible influence of uncertain variables on the evolution of the clogging rate τ_c
- Identify the possible key drivers of the high clogging rate

Table of contents

- 1. Introduction**
- 2. Physics and numerics of the clogging phenomenon in SGs**
- 3. Uncertainty quantification and propagation in the TPD chain**
- 4. Variance-based GSA using PCE**
- 5. Kernel-based given data SA**
- 6. Conclusion**

2. Clogging For Dummies

Physics and numerics of the clogging phenomenon in SGs

◆ Overview of the physical modeling

- The main system of equations (mixed 2 PDE + 1 ODE) can be given by:

$$\begin{cases} \partial_t \tilde{\Gamma}_p + U_\ell \cdot \nabla \tilde{\Gamma}_p = f_p(\Phi_p, \Phi_s, \tilde{\Gamma}_p, \Gamma_s^{\max}) \\ \partial_t \tilde{\Gamma}_s + U_\ell \cdot \nabla \tilde{\Gamma}_s = f_s(\Phi_p, \Phi_s, \tilde{\Gamma}_s, \Gamma_s^{\max}) \\ \frac{dm_c}{dt} = \Phi_p + \Phi_s \\ \Gamma_s(0, .) = \Gamma_s(0), \quad \Gamma_p(0, .) = \Gamma_p(0) \end{cases} \quad (1)$$

where:

- for $u = \{s, p\}$, one has $\tilde{\Gamma}_u = \rho_m C_\ell \Gamma_u$ and where f_u are essentially additive functions of their variables
- ρ_m , C_ℓ and U_ℓ ↳ (resp.) density of the liquid-gas mixture, liquid quality, velocity of the liquid phase
- mass fractions Γ_p, Γ_s of iron oxides in the different chemical states (solid particles and soluble particles, respectively)
- solubility map of iron oxide Γ_s^{\max} + initial conditions $\Gamma_p(0), \Gamma_s(0)$
- mass of iron oxide m_c w.r.t. fluxes Φ_p, Φ_s

Physics and numerics of the clogging phenomenon in SGs

◆ Vena contracta

As for the particle flux related to the vena contracta mechanism which is of interest here, it is given by [Pru12]:

$$\Phi_p = \textcolor{red}{a_v} \frac{k_v (\rho_p - \rho_\ell) U_z^2 d_p^2}{\mu_\ell} \tilde{\Gamma}_p \quad (2)$$

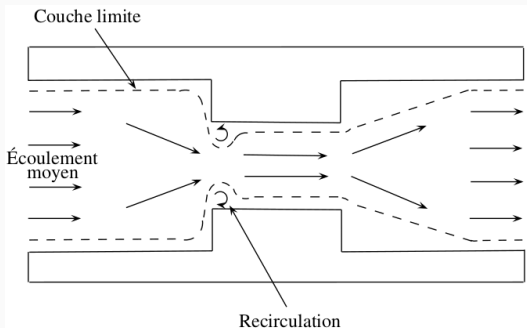


Figure 5: Illustration of the *vena contracta* mechanism.

◆ Clogging rate calculation

- Finally, τ_c is obtained through the following empirical correlation:

$$\tau_c = \alpha (1 - \exp\{-\beta V_c\}) . \quad (3)$$

- Two other chemical phenomena are of interest:
 - Chemical conditioning of the circuit
 - Chemical cleaning procedures

Physics and numerics of the clogging phenomenon in SGs

◆ Summary

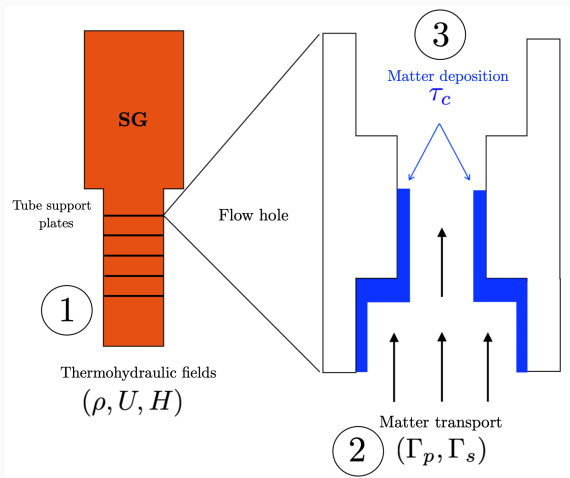


Figure 6: Summary of the clogging rate calculation.

Physics and numerics of the clogging phenomenon in SGs

◆ Overview of the numerical model

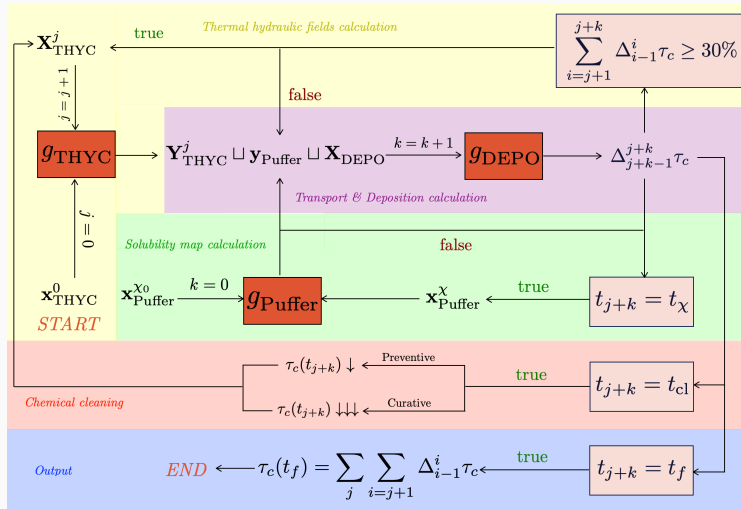


Figure 7: THYC-Puffer-DEPO code architecture.

3. UQ in the TPD chain

Uncertainty quantification and propagation in the TPD chain

◆ Uncertainty quantification

- $d = 7$ independent input variables:

$$\mathbf{X}_{\text{DEPO}} := (\alpha, \beta, \epsilon_e, \epsilon_c, d_p, \Gamma_p(0), a_v)^\top \sim \mathbb{P}_{\mathbf{X}_{\text{DEPO}}} \quad (4)$$

- Output Vol \Rightarrow clogging rate increment between two instants $t < t'$

$$\Delta_t^{t'} \tau_c := \tau_c(t') - \tau_c(t) \quad (5)$$

Variable	Signification	Distribution
α	First empirical correlation parameter	$\mathcal{N}(101.6, 4.0)$
β	Second empirical correlation parameter	$\mathcal{N}(0.0233, 0.0005)$
ϵ_e	Porosities of the fouling deposits	$\mathcal{T}(0.2, 0.3, 0.5)$
ϵ_c	Porosities of the clogging deposits	$\mathcal{T}(0.01, 0.05, 0.3)$
d_p	Iron oxide particle diameter (m)	$\mathcal{T}(0.5, 5.0, 10.0) \times 10^{-6}$
$\Gamma_p(0)$	Initial data for solid particles mass fraction transport equation	$\mathcal{T}(1.0, 4.5, 8.0) \times 10^{-9}$
a_v	Calibration parameter of the <i>vena contracta</i> physical mechanism	$\mathcal{T}(0.1, 7.8, 12) \times 10^{-4}$

- Numerical procedure:

- Scenario: for a specific SG, simulate over $[0, t_f = 50]$ years
- $n = 10^3$ Monte Carlo simulations (in // using HPC facility)
- 1 call ≈ 5 hours

Uncertainty quantification and propagation in the TPD chain

◆ Uncertainty propagation using Monte Carlo simulations

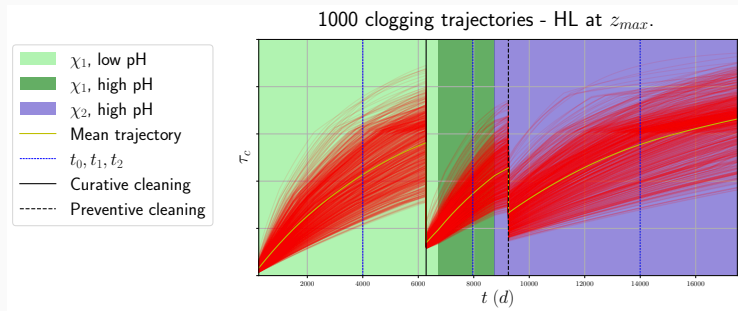


Figure 8: Trajectories obtained from Monte Carlo simulations (with curative and preventive chemical cleanings).

Uncertainty quantification and propagation in the TPD chain

◆ Uncertainty propagation using Monte Carlo simulations

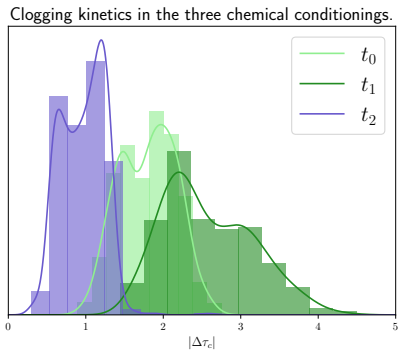


Figure 9: Densities of clogging kinetics for various chemical regimes.

Uncertainty quantification and propagation in the TPD chain

◆ Uncertainty propagation using Monte Carlo simulations

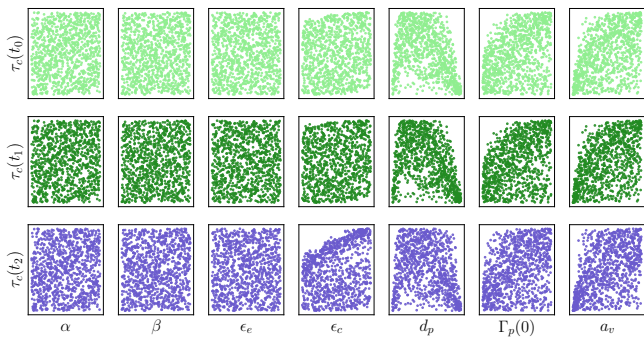


Figure 10: Scatter plots in the rank-space for the three different chemical conditionings.

4. GSA with PCE

Variance-based GSA using PCE

◆ Surrogate modeling using Polynomial Chaos Expansions (PCE)

- ❑ Problem considered here:
 - Output variable of interest is time-dependent
 - g is costly
 - X is relatively low dimensional
- ❑ Surrogate modeling strategy \Rightarrow Polynomial Chaos Expansions (PCE)
- ❑ Known advantages / drawbacks (compared to other types of surrogates)
 - ✓ PCE coefficients can be used to interpret the underlying structure of the model
 - ✓ Sobol' indices are an analytical byproduct of the method
 - ✗ PCE does not provide any intrinsic prediction intervals (neither on the output nor on the Sobol' indices)
 - ✗ Tuning p (polynomial degree) and the q -norm can be tricky

Variance-based GSA using PCE

◆ Time-dependent surrogate modeling with PCE... in a nutshell

- Clogging rate output:

$$g : (t, z, \mathbf{X}) \in [0, t_f] \times [0, z_{\max}] \times \mathcal{X} \mapsto g(t, z, \mathbf{X}) \in [0, 100] , \quad (6)$$

where $\mathbf{X} := \mathbf{X}_{\text{DEPO}} \in \mathcal{X} = \mathcal{X}_1 \times \dots \times \mathcal{X}_d \subset \mathbb{R}^d \sim \mathbb{P}_{\mathbf{X}}$

- For a choice of inputs \mathbf{X}_0 , the output is a function $(t, z) \mapsto g(t, z, \mathbf{X}_0)$
- Results will be considered at the specific altitude $z_{\max} \Leftrightarrow$ top of the highest TSP in the hot leg of the SG
- Time discretization N (such that $t_N = t_f$):

$$\left(g(t_1, z_{\max}, \mathbf{X}_0), \dots, g(t_N, z_{\max}, \mathbf{X}_0) \right) \in \mathbb{R}^N \quad (7)$$

◆ Time-dependent surrogate modeling with PCE... in a nutshell

- Hilbert basis $\{\varphi_\alpha\}_\alpha \in \mathbb{N}^d$ of tensorized orthonormal polynomials (Wiener-Askey PCE scheme + Adaptive Stieltjes algorithm)
- At each time step, the PCE of highest degree $p \in \mathbb{N}$ is constructed as:

$$\tilde{g}(\mathbf{X}) = \sum_{\alpha \in \mathcal{J}} g_\alpha \varphi_\alpha(\mathbf{X}), \quad (8)$$

where:

- $g_\alpha = (g_\alpha(t_1), \dots, g_\alpha(t_N)) \in \mathbb{R}^N$ for all
 $\alpha \in \mathcal{J} \subseteq \{\alpha \in \mathbb{N}^d, \sum_{i=1}^d |\alpha_i| \leq p\}$
- Components of the coefficient vector: $g_\alpha^k := g_\alpha(t_k)$
- Index set: $\mathcal{J} = \mathcal{J}_1 \cup \dots \cup \mathcal{J}_N$ determined $\forall t_k, k \in \{1, \dots, N\}$
 - ▷ two-step method (hyperbolic enumeration rule + LARS)

Variance-based GSA using PCE

◆ Time-dependent surrogate modeling with PCE... in a nutshell

- Validation of the surrogate model \Leftrightarrow predictivity coefficient Q^2
- Test dataset: $\mathcal{D}^{\text{test}} = \{(\mathbf{X}_j^{\text{test}}, g(t_k, \mathbf{X}_j^{\text{test}}))\}_{k,j \in \{1, \dots, N\} \times \{1, \dots, m\}}$ of size $m < n$ at every time discretization (t_1, \dots, t_N) over $[0, t_N]$
- Metrics: $\forall k \in \{1, \dots, N\}$,

$$Q^2(t_k) := 1 - \sum_{j=1}^m \frac{|g(t_k, \mathbf{X}_j^{\text{test}}) - \sum_{\alpha \in \mathcal{J}_k} g_\alpha^k \varphi_\alpha(\mathbf{X}_j^{\text{test}})|^2}{\text{Var}(g(t_k, \mathbf{X}_j^{\text{test}}))} \quad (9)$$

$$\overline{Q^2} := \frac{1}{N} \sum_{k=1}^N Q^2(t_k) \quad (10)$$

- Hyperparameters? \Leftrightarrow Find degree p and q -norm s.t. $\overline{Q^2}$ is maximized!

Variance-based GSA using PCE

◆ Time-dependent surrogate modeling with PCE... in a nutshell

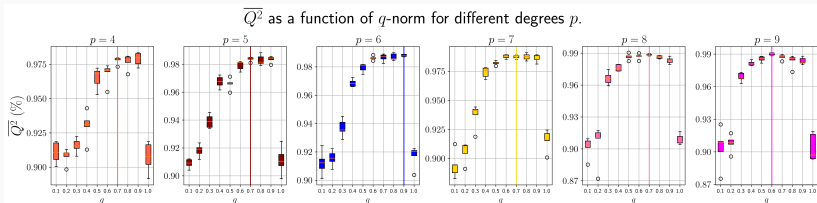


Figure 11: Time-averaged predictivity coefficient of PCE expansions of different degrees p and different choices of q -norm.

- ☛ Max degree of $p = 7$
- ☛ Hyperbolic rule with $q = 0.7$

Variance-based GSA using PCE

◆ Time-dependent surrogate modeling with PCE... in a nutshell

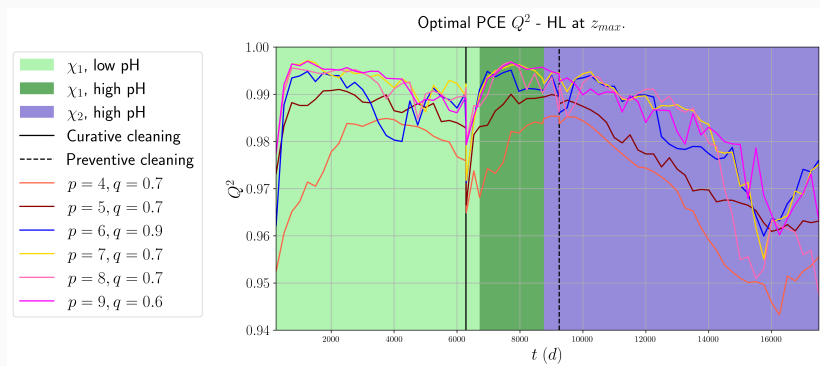


Figure 12: Time-variation of the predictivity coefficient for PCEs with (p, q) -hyperparameters maximizing the $\overline{Q^2}$.

- ☒ Max degree of $p = 7$
- ☒ Hyperbolic rule with $q = 0.7$

Variance-based GSA using PCE

◆ Time-dependent Sobol' indices with PCE

□ Functional ANOVA:

$$g^k(\mathbf{X}) = \sum_{\gamma \subseteq \{1, \dots, d\}} g_\gamma^k(X_{\gamma_1}, \dots, X_{\gamma_d}) = \sum_{\gamma \subseteq \{1, \dots, d\}} g_\gamma^k(\mathbf{X}_\gamma) \quad (11)$$

□ Time-dependent Sobol' indices:

$$S_\gamma(t_k) = \frac{\sum_{\alpha \in \mathcal{J}_\gamma} (g_\alpha^k)^2}{\sum_{1 \leq |\alpha| \leq p} (g_\alpha^k)^2} \quad (12)$$

□ In practice, we calculate:

$$S_i(t_k) = \frac{\text{Var}(g_i^k(X_i))}{\text{Var}(g^k(\mathbf{X}))} \quad (\text{first-order}) \quad (13)$$

$$S_i^T(t_k) = \sum_{\gamma | i \subset \gamma} S_\gamma(t_k) \quad (\text{total}) \quad (14)$$

$$S_*(t_k) = 1 - \sum_{i=1}^d S_i(t_k) \quad (\text{interaction}) \quad (15)$$

Variance-based GSA using PCE

◆ Variance-based GSA on the TPD case

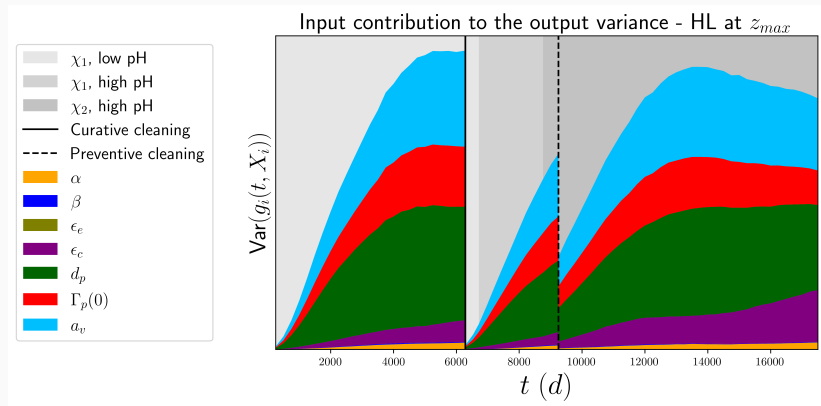


Figure 13: Evolution of the variance contribution of each uncertain input for $i \in \{1, \dots, d\}$

Variance-based GSA using PCE

◆ Variance-based GSA on the TPD case

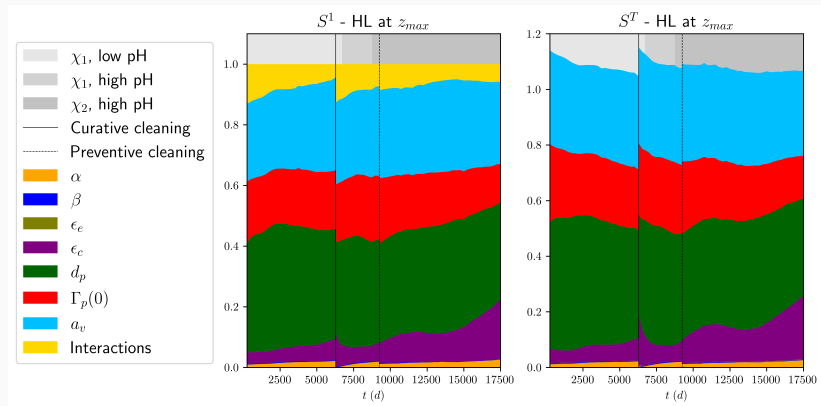


Figure 14: Evolution of first-order, interactions (left) and total-order (right) time-dependent Sobol' indices.

5. SA with HSIC

Kernel-based given data SA

◆ HSIC in a nutshell (one slide!)

- HSIC \Leftrightarrow Hilbert-Schmidt Independence Criterion
- Relies on kernel mean embedding of probability distributions
- By choosing suited kernels (*characteristic kernels*) on the inputs and output and using a dedicated divergence metric (*Maximum Mean Discrepancy*)
 - \Leftrightarrow **allows to** $\mathbb{P}_{(Y, X_i)}$ **vs.** $\mathbb{P}_{(Y \times X_i)}$
- A fundamental property:

$$\text{HSIC}(X_i, Y) = 0 \iff X_i \perp Y \quad (16)$$

- Tools in practice:
 - \Leftrightarrow estimators (U-stat, V-stat), normalized indices, three types of studies (global, target, conditional), statistical independence tests
- For a nice introduction about this wonderful topic:
 - \Leftrightarrow cf. Talk by A. Marrel (+ V. C. and J. P.) @ OT Users' Day #14 (2021)
 - \Leftrightarrow OT doc: here!

Kernel-based given data SA

◆ Global analysis using HSIC indices on the TPD case

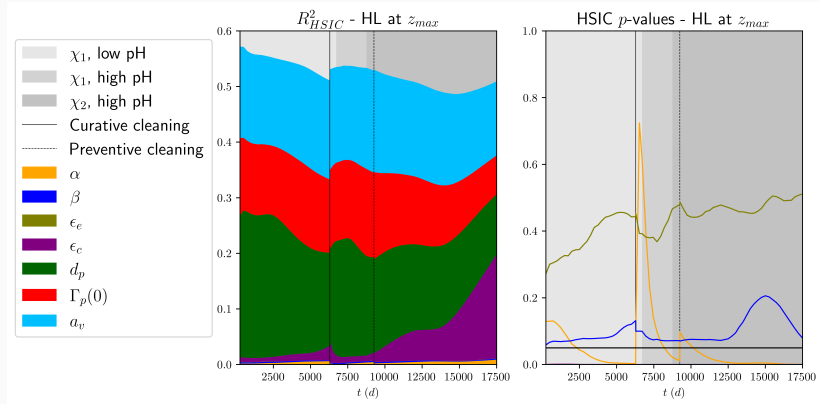


Figure 15: Time-dependent R^2 -HSIC indices and associated p -values ($\alpha = 5\%$).

Kernel-based given data SA

◆ Target analysis using T-HSIC indices on the TPD case

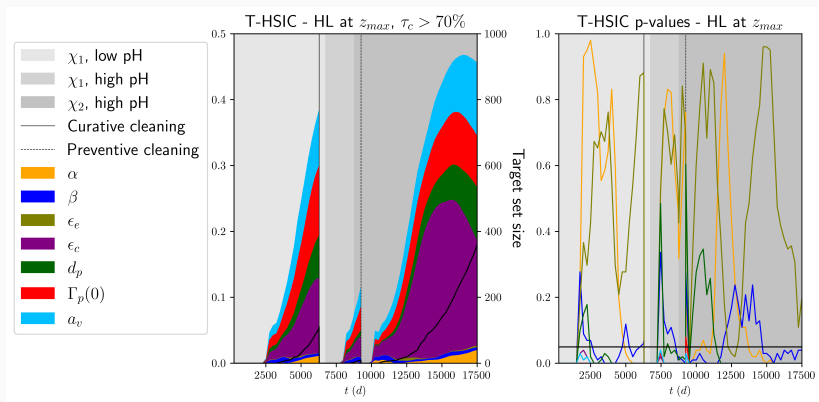


Figure 16: Time-dependent T-HSIC indices and associated p -values ($\alpha = 5\%$).

☞ ! The threshold 70% has been chosen for illustrative purposes but does not reflect real operating conditions.

Kernel-based given data SA

◆ Conditional analysis using C-HSIC indices on the TPD case

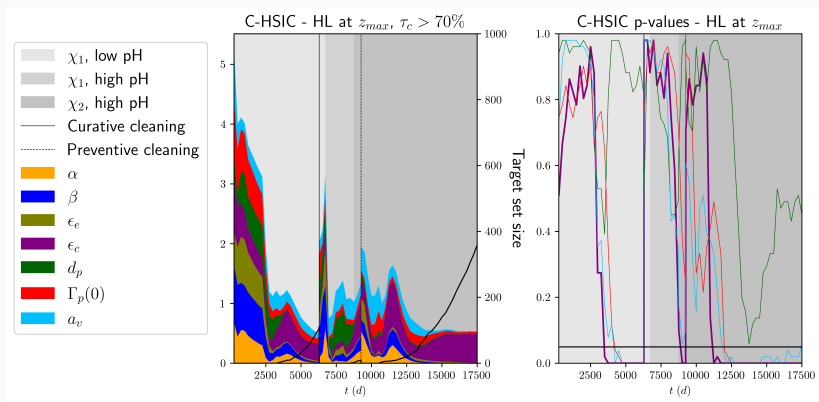


Figure 17: Time-dependent C-HSIC indices and associated p -values ($\alpha = 5\%$).

☞ ! The threshold 70% has been chosen for illustrative purposes but does not reflect real operating conditions.

Conclusion

Conclusion

◆ A few take-home messages

- ✓ All in all \Rightarrow we recover qualitative results that align with [LSS⁺23]
- ✓ PCE surrogate model \Rightarrow rather predictive + reveals that the interactions between inputs are relatively weak, resulting in a quasi-additive structure of the underlying model
- ✓ SA results \Rightarrow new influential variables detected (global, target, conditional) using both Sobol' and HSIC indices

☞ Main contributions ☞

- ❑ Article: IJUQ / HAL / ArXiv
- ❑ Repository: EdgarJaber/SA-for-clogging-code

Conclusion

◆ A few perspectives

- Use the new OT functionalities adapted to field surrogate modeling
- Investigate other classes of metamodels, especially adapted to functional behavior in output (e.g., ↗ [SSW15, LRG⁺23])
- Investigate other types of kernels for HSIC-based SA adapted to functional outputs ↗ [EAM24]
- Provide prediction intervals for surrogate models using the Conformal Prediction framework ↗ [JVB⁺24]
- Perform Bayesian calibration of the computer model w.r.t. in-situ data (↗ ongoing work)

Thank you for your attention!
Any question?

References i

-  R. El Amri and A. Marrel.
More powerful HSIC-based independence tests, extension to space-filling designs and functional data.
International Journal for Uncertainty Quantification, 14:69–98, 2024.
-  Q. Feng, J. Nebes, M. Bachet, S. Pujet, D. You, and E. Deri.
Tube support plates blockage of PWR steam generators: thermalhydraulics and chemical modeling.
Proceedings of the International Conference on Water Chemistry in Nuclear Reactor Systems (NPC 2023), Juan-les-Pins, September 2023.
-  S. Girard.
Diagnostic du colmatage des générateurs de vapeur à l'aide de modèles physiques et statistiques.
PhD thesis, École Nationale Supérieure des Mines de Paris, 2012.
-  E. Jaber, Blot V., N. Brunel, V. Chabridon, E. Remy, B. Iooss, D. Lucor, M. Mougeot, and A. Leite.
Conformal Approach To Gaussian Process Surrogate Evaluation With Coverage Guarantees.
Preprint, 2024.
-  N. Lüthen, O. Roustant, F. Gamboa, B. Iooss, S. Marelli, and B. Sudret.
Global sensitivity analysis using derivative-based sparse Poincaré Chaos Expansions.
International Journal for Uncertainty Quantification, 13:57–82, 2023.
-  L. Lefebvre, M. Segond, R. Spaggiari, L. Le Gratiet, E. Deri, B. Iooss, and G. Damblin.
Improving the Predictivity of a Steam Generator Clogging Numerical Model by Global Sensitivity Analysis and Bayesian Calibration Techniques.
Nuclear Science and Engineering, 197(8):2136–2149, 2023.
-  T. Prusek.
Modélisation et simulation numérique du colmatage à l'échelle du sous-canal dans les générateurs de vapeur.
Thèse de l'Université Aix-Marseille, 2012.

References ii



R. Schöbi, B. Sudret, and J. Wiart.

Polynomial-Chaos-based Kriging.

International Journal for Uncertainty Quantification, 5:171–193, 2015.